LETTERS
PUBLISHED ONLINE: 24 JUNE 2012 | DOI: 10.1038/NPHOTON.2012.124
nature photonics

Experimental realization of three-dimensional indefinite cavities at the nanoscale with anomalous scaling laws

Xiaodong Yang[1,2†], Jie Yao[2†], Junsuk Rho[2†], Xiaobo Yin[1,2] and Xiang Zhang[1,2*]

Metamaterials allow for extraordinary electromagnetic properties that are not attainable in nature[1–9]. Indefinite media with hyperbolic dispersion, in particular, have found intriguing applications[10–13]. The miniaturization of optical cavities increases the photon density of states and therefore enhances light–matter interactions for applications in modern optoelectronics. However, scaling down the optical cavity is limited to the diffraction limit and by the reduced quality factor. Here, we experimentally demonstrate an optical cavity made of indefinite metamaterials that confines the electromagnetic field to an extremely small space. The experiments reveal that indefinite cavities demonstrate anomalous scaling laws: cavities with different sizes can resonant at the same frequency, and a higher-order resonance mode oscillates at a lower frequency. We also demonstrate a universal fourth power law for the radiation quality factor of the wave vector. Cavities with sizes down to $\lambda/12$ are realized with ultrahigh optical indices (up to 17.4), a feature that is critically important for many applications[14–18].

The strong optical field confinement in optical cavities such as microspheres, microtoroids and photonic-crystal cavities[19–21] has led to numerous exciting applications in areas including integrated photonics, nonlinear optics, quantum electrodynamics and optomechanics[22–25]. Owing to the limited refractive indices of naturally available materials, the physical sizes of these cavities are limited to the wavelength scale for efficient light confinement. Most recently, metamaterials with an ultrahigh refractive index (in the terahertz regime) have been explored[26–28]. However, the experimental implementation of such a metamaterial at optical frequencies is difficult because of fabrication constraints. Another approach for achieving nanoscale optical cavities that makes use of nanowire metamaterials has been theoretically investigated[29]. In this Letter, we experimentally demonstrate metal–dielectric multilayer indefinite metamaterials with optical refractive indices as large as 17.4, which is far beyond that found in natural materials. With such a high optical index, three-dimensional optical cavities with dimensions down to $\lambda/12$ and unprecedented properties are demonstrated. Unlike conventional microcavities in which the resonant frequencies depend strongly on size, indefinite cavities support exactly the same resonant frequency in cavities with drastically different sizes as the result of their size-dependent effective indices. The indefinite cavity is found to scale anomalously such that a higher-order mode will resonate at a lower frequency. In contrast to the commonly held principle, the radiation quality factors of the cavities scale inversely with cavity size, and we find experimentally that there is a universal fourth power law between the radiation quality factor and the resonating wave vector.

The metamaterial structure consists of alternating thin layers of silver and germanium (Fig. 1a). When the multilayer period is much less than the wavelength, the multilayer can be considered as an effective medium described by Maxwell–Garnet theory (Supplementary Section S2). The permittivity tensor of such metamaterials is uniaxial and the real parts of its principal components can have different signs, resulting in a three-dimensional hyperboloid iso-frequency contour (IFC) (Fig. 1b). A spherical IFC of air with radius k_0 is plotted for comparison ($k_0 = 2\pi/\lambda_0$). As a result of the open-curved hyperboloid dispersion, the indefinite medium allows a wave with an extremely large wave vector to propagate, and the giant momentum mismatch between the metamaterial and the air causes total internal reflection (TIR) at the interface (Supplementary Section S3). By cutting the metamaterial into a subwavelength cube, a three-dimensional optical Fabry–Pérot cavity can be formed with an effective refractive index given by $n_{\mathrm{eff}} = k/k_0$. Because, theoretically, extremely large wave vectors can be achieved along the unbound IFC hyperboloid, the cavity size can be squeezed into a nanometre scale.

Figure 2 shows the calculated cavity modes in indefinite optical cavities. The cross-section of the IFC at 150 THz was obtained from a spatial Fourier analysis of finite-difference time-domain (FDTD) calculations, which matches the effective medium calculation well (Fig. 2a). It is clear that the five cavities with different size combinations (width, height) support identical optical modes with the same resonant frequency and the same mode order $(m_x,m_y,m_z) = (1,1,1)$ (Fig. 2b). The resonating wave vectors of these cavity modes locate on the same hyperbolic IFC in Fig. 2a. For conventional optical cavities made of natural materials, the resonant frequency of a cavity mode is strongly dependent on cavity size because the available wave vector is limited to a circular or elliptical IFC in isotropic or anisotropic materials. In contrast, indefinite cavities with drastically different sizes resonate at an identical frequency as long as the resonating wave vectors share the same IFC. This is due to the fact that, when the cavity scales down, the resonating wave vector increases along the unbounded hyperbolic dispersion. For example, an optical cavity with size (width,height) of (45,30) nm, equivalent to $(\lambda/44,\lambda/67)$, supports a wave vector of $k = 39.5k_0$ for the (1,1,1) mode, which corresponds to $n_{\mathrm{eff}} = 39.5$. Furthermore, among the first five eigenmodes along the z-direction for a cavity with dimensions of (160,150) nm (Fig. 2c), the higher-order mode is found at a lower resonant frequency, displaying anomalous dispersion in relation to the mode orders due to the opposite signs of the principal components of the permittivity tensor. Such behaviour is also observed when using the effective medium calculation (Supplementary Fig. S2).

[1]Materials Sciences Division, Lawrence Berkeley National Laboratory, 1 Cyclotron Road, Berkeley, California 94720, USA, [2]NSF Nano-scale Science and Engineering Center (NSEC), 3112 Etcheverry Hall, University of California at Berkeley, Berkeley, California 94720, USA; †These authors contributed equally to this work. *e-mail: xiang@berkeley.edu

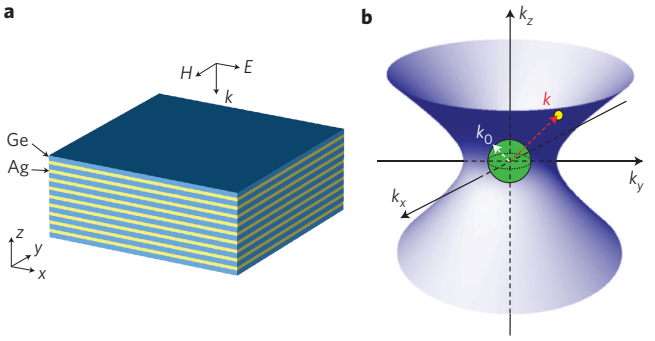

Figure 1 | Schematic of multilayer indefinite metamaterial structure and its hyperboloid IFC. a, Indefinite metamaterial with alternating silver and germanium multilayers. The permittivity components are negative along the *x*- and *y*-directions and positive along the *z*-direction (obtained from effective medium theory). A three-dimensional indefinite optical cavity can be created based on TIR at the interface between the metamaterial and air. **b**, Hyperboloid IFC of the multilayer metamaterial calculated from the dispersion relation (blue surface) and the spherical isotropic IFC of air with radius k_0 (green surface). The yellow dot located on the hyperboloid shows the resonating wave vector k inside the cavity, which is much larger than k_0, indicating an ultrahigh effective refractive index $n_{eff} = k/k_0$.

The metamaterial cavities were fabricated by alternating layers of silver and germanium (thicknesses of 20 nm and 30 nm, respectively). A scanning electron microscope (SEM) image of cavity arrays (dimensions, (170,150) nm) consisting of three pairs of silver–germanium multilayers, as well as close views of three cavities of different sizes, are shown in Fig. 3a,b. The side walls of the cavities are tilted (~75°) as a result of the lift-off process in the electron-beam lithography step. FDTD simulations found that cavity modes still exist in cavities with tilted side walls, although the resonant frequencies shift higher (Supplementary Section S6). The cavity modes were excited with a plane wave propagating along the *z*-direction, with *x*-direction polarization for the transmission measurement in Fourier-transform infrared (FTIR) spectroscopy. Figure 3c shows that the cavities with different sizes resonate at the same resonant frequency for the (1,1,1) modes. This phenomenon was observed for all three different resonance frequencies. It can be understood that, as the cavity size shrinks, both k_x and k_z scale up simultaneously along the same IFC to maintain the cavity resonant frequency. The indefinite cavities therefore have size-dependent refractive indices, a unique feature that does not exist in conventional optical cavities where the refractive index is not strongly related to the cavity size and a larger cavity has a lower resonant frequency for a given mode order. Also, for a given cavity, the (1,1,2) mode has a lower resonant frequency than the (1,1,1) mode, thereby demonstrating the anomalous mode dispersion. When the mode order increase along the *z*-direction, a significant increase in k_z causes the higher-order mode to oscillate on a flatter IFC with a lower frequency (Supplementary Fig. S6). In contrast, in conventional optical cavities, the normal mode dispersion entails a higher resonating frequency for a higher-order mode in a given cavity. The measured resonating wave vectors for our indefinite cavities agree well with the calculated IFCs (Supplementary Fig. S6).

By measuring the full-width at half-maximum (FWHM) of the resonance peaks in Fig. 3c, a total quality factor Q_{tot} of ~4 was obtained for all cavity modes, which is dominated by the absorption in the metal, as $1/Q_{tot} = 1/Q_{rad} + 1/Q_{abs}$, where Q_{rad} and Q_{abs} are the quality factors from radiation and absorption, respectively. Although the resonance peaks have similar widths, the transmission depths for each cavity mode are different, which is related to the radiation coupling strength between the excitation plane wave and

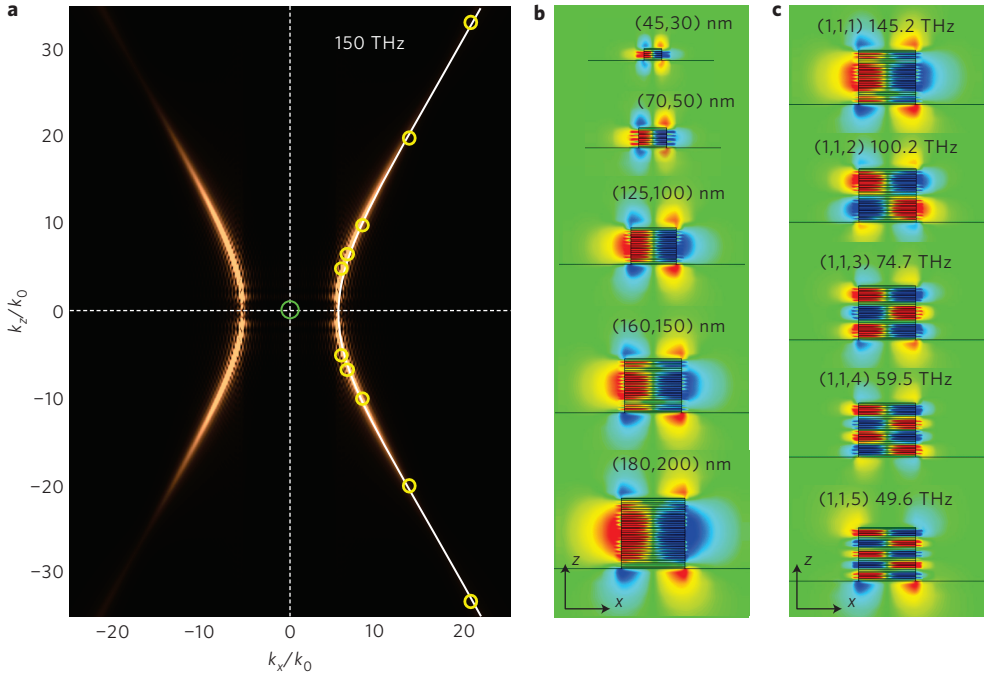

Figure 2 | FDTD-calculated IFC of the multilayer metamaterial and mode profiles of indefinite optical cavities. a, Cross-sectional view of the hyperbolic IFC for 4 nm silver and 6 nm germanium multilayer metamaterial at 150 THz (bronze curve), which matches the effective medium calculation (white line). The yellow circles represent the resonating wave vectors of the cavity modes shown in **b**, and the green circle represents the light cone of air. **b**, FDTD-calculated electric field (E_z) distributions of the (1,1,1) mode for cavities made of 4 nm silver and 6 nm germanium multilayer metamaterial with different size (width, height) combinations but at the same resonant frequency of 150 THz. **c**, FDTD-calculated E_z distributions of the first five cavity modes along the *z*-direction for the (160,150) nm cavity.

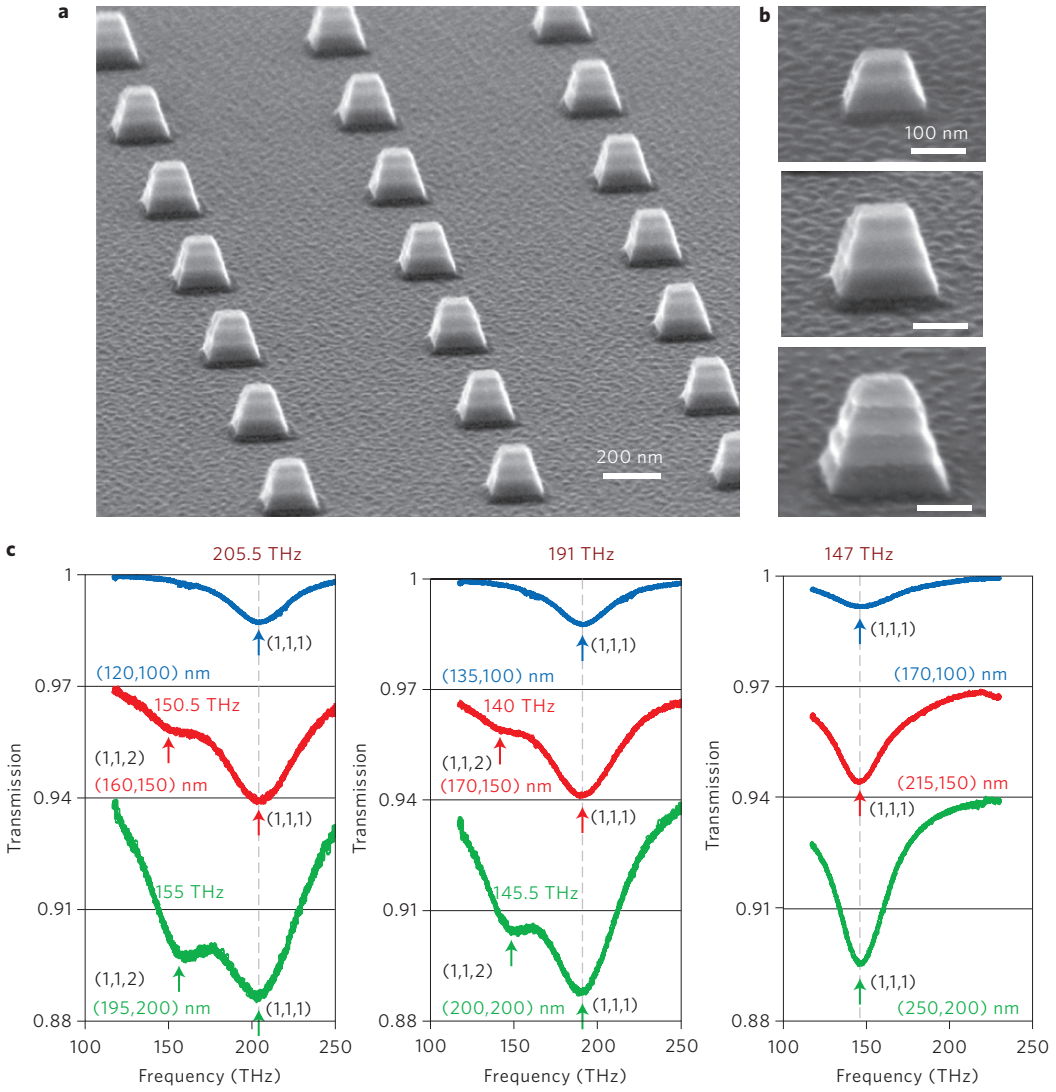

Figure 3 | SEM images and measured transmission spectra of indefinite optical cavities with different sizes. a, SEM image (perspective view) of an indefinite optical cavity array (cavity size, (170,150) nm), with multilayers of 20 nm silver and 30 nm germanium clearly visible. **b**, SEM images of three cavities with different dimensions — (135,100) nm, (170,150) nm and (200,200) nm—with two, three and four pairs of silver/germanium multilayers, respectively. **c**, FTIR measured transmission spectra through an indefinite optical cavity array with a 5% cavity area filling ratio for cavities of different sizes. The three panels correspond to cavities located at three different IFCs for (1,1,1) modes with resonant frequencies of 205.5, 191 and 147 THz, respectively.

the cavity mode. It can be seen that the transmission depths are shallower for smaller cavities with the same mode order, and higher-order modes transmit more light (Fig. 3c). This indicates that the radiation coupling strength is strongly dependent on cavity size and mode order, which is determined by the resonating wave vector. As illustrated in Fig. 2a, for a smaller cavity, the resonating wave vector is further from the IFC of air, so radiation coupling between the cavity mode and the incident plane wave is weaker due to the increased momentum mismatch. The hyperbolic dispersion of an indefinite medium supports very large wave vectors, so the radiative loss of such cavities is strongly suppressed.

To measure the Q_{rad} of the cavity modes, the absorption loss of the metal has to be isolated. We used coupled mode theory[30,31] to retrieve the vertical coupling radiation quality factors $Q_{rad,\nu}$ between the plane wave and the cavity modes within a unit waveguide channel based on the measured transmission spectra from the cavity array (Supplementary Sections S4,S8). We found a universal fourth power law between $Q_{rad,\nu}$ and k: that is, $Q_{rad,\nu} \approx (k/k_0)^4$ or n_{eff}^4, for all cavities of different height, width, mode order and resonant frequency (Fig. 4a). Because the wave vector is proportional to the mode order divided by the cavity size, a smaller cavity or higher-mode order has a higher $Q_{rad,\nu}$ arising from the larger momentum mismatch. Although the experiment measured $Q_{rad,\nu}$, the FDTD calculation shows that the total radiation quality factor Q_{rad} also follows the fourth power law, giving $Q_{rad} \approx (k/k_0)^4$ (Fig. 4b). Such a universal scaling law can be understood by the fact that Q_{rad} is proportional to n_{eff}/α_{rad}, where α_{rad} is the radiation loss of the cavity mode due to TIR. The radiated power can be represented as the integral of the k-space distribution of the cavity mode over the light cone of air in three dimensions, so that α_{rad} is proportional to k^{-3} (refs 32,33). Because n_{eff} is proportional to k, Q_{rad} therefore increases as the fourth power of k (Supplementary Fig. S13). This unique behaviour of Q_{rad} in the indefinite cavity is very different from that in conventional dielectric optical cavities with dimensions on a scale larger than the wavelength, such as in microspheres and microdisks, where the TIR-induced Q_{rad} decreases when the cavity becomes smaller due to the larger surface curvature leading to increased radiation leakage

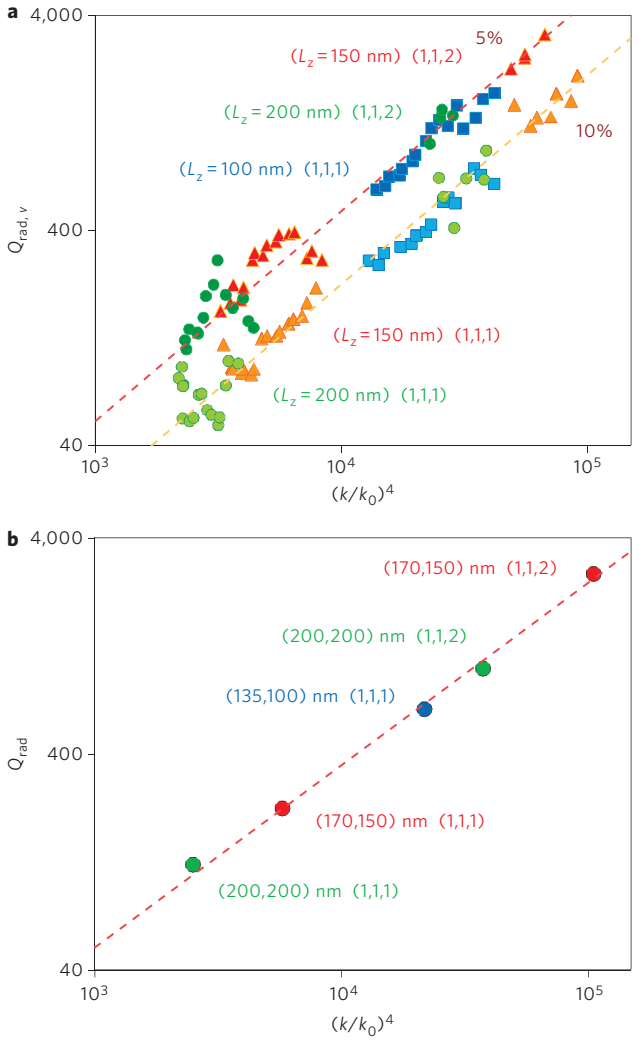

Figure 4 | Radiation quality factor as a function of the resonating wave vector of a cavity mode. a, The retrieved vertical radiation quality factor $Q_{rad,v}$ scales as $(k/k_0)^4$ or n_{eff}^4, a universal fourth power law, for cavities with different dimensions, resonance frequencies and mode orders. The cavity sizes investigated include (~110–185,100) nm, (~140–215,150) nm and (~185–255,200) nm for the (1,1,1) mode, and (~140–170,150) nm and (~185–210,200) nm for the (1,1,2) mode. Cavity area filling ratios of 5% and 10% are considered. **b**, FDTD-calculated total radiation quality factor Q_{rad} of a single cavity shows the same power law. The dashed lines are fitting lines for the coloured dots.

into the light cone of air. The indefinite cavities also allow an unnaturally high refractive index, and a maximum value of 17.4 is obtained for the (1,1,2) modes shown in Fig. 4a.

The demonstrated three-dimensional nanoscale optical cavities made of indefinite metamaterials have unprecedented anomalous scaling laws, which are drastically different from conventional cavities made of natural materials. In contrast to conventional cavities in which the size is limited to the wavelength scale, indefinite cavities can be scaled down to extremely deep subwavelength sizes at exactly the same resonant frequency due to their size-dependent effective refractive indices. As cavity size reduces, the radiation quality factor increases dramatically, following the fourth power scaling law of the resonating wave vector resulting from the hyperbolic dispersion of the indefinite medium. These unique properties of indefinite cavities will significantly increase the photon density of states and therefore enhance light–matter interactions. Such indefinite cavities therefore open up new possibilities for nanophotonic applications in cavity quantum electrodynamics, optical nonlinearities, optomechanics, biosensing and optical communications.

Received 25 October 2011; accepted 24 April 2012; published online 24 June 2012

References

1. Smith, D. R., Pendry, J. B. & Wiltshire, M. C. K. Metamaterials and negative refractive index. *Science* **305,** 788–792 (2004).
2. Veselago, V. G. The electrodynamics of substances with simultaneously negative values of ε and μ. *Sov. Phys. Usp.* **10,** 509–514 (1968).
3. Pendry, J. B., Holden, A. J., Robbins, D. J. & Stewart, W. J. Magnetism from conductors and enhanced nonlinear phenomena. *IEEE Trans. Microw. Theory Tech.* **47,** 2075–2084 (1999).
4. Shelby, R. A., Smith, D. R. & Schultz, S. Experimental verification of a negative index of refraction. *Science* **292,** 77–79 (2001).
5. Valentine, J. *et al.* Three-dimensional optical metamaterial with a negative refractive index. *Nature* **455,** 376–379 (2008).
6. Pendry, J. B., Schrurig, D. E. & Smith, D. R. Controlling electromagnetic fields. *Science* **312,** 1780–1782 (2006).
7. Schurig, D. *et al.* Metamaterial electromagnetic cloak at microwave frequencies. *Science* **314,** 977–980 (2006).
8. Cai, W. S., Chettiar, U. K., Kildishev, A. V. & Shalaev, V. M. Optical cloaking with metamaterials. *Nature Photon.* **1,** 224–227 (2007).
9. Valentine, J., Li, J. S., Zentgraf, T., Bartal, G. & Zhang, X. An optical cloak made of dielectrics. *Nature Mater.* **8,** 568–571 (2009).
10. Smith, D. R. & Schurig, D. Electromagnetic wave propagation in media with indefinite permittivity and permeability tensors. *Phys. Rev. Lett.* **90,** 077405 (2003).
11. Jacob, Z., Alekseyev, L. V. & Narimanov, E. Optical hyperlens: far-field imaging beyond the diffraction limit. *Opt. Express* **14,** 8247–8256 (2006).
12. Salandrino, A. & Engheta, N. Far-field subdiffraction optical microscopy using metamaterial crystals: theory and simulations. *Phys. Rev. B* **74,** 075103 (2006).
13. Liu, Z., Lee, H., Xiong, Y., Sun, C. & Zhang, X. Far-field optical hyperlens magnifying sub-diffraction-limited objects. *Science* **315,** 1686 (2007).
14. Mansfield, S. M. & Kino, G. S. Solid immersion microscope. *Appl. Phys. Lett.* **57,** 2615–2616 (1990).
15. Xiong, Y., Liu, Z. & Zhang, X. Projecting deep-subwavelength patterns from diffraction-limited masks using metal–dielectric multilayers. *Appl. Phys. Lett.* **93,** 111116 (2008).
16. Shi, Z. *et al.* Slow-light Fourier transform interferometer. *Phys. Rev. Lett.* **99,** 240801 (2007).
17. Han, S. *et al.* Ray optics at a deep-subwavelength scale: a transformation optics approach. *Nano Lett.* **8,** 4243–4247 (2008).
18. Zentgraf, T., Liu, Y., Mikkelsen, M. H., Valentine, J. & Zhang, X. Plasmonic Luneburg and Eaton lenses. *Nature Nanotech.* **6,** 151–155 (2011).
19. Spillane, S. M., Kippenberg, T. J. & Vahala, K. J. Ultralow-threshold Raman laser using a spherical dielectric microcavity. *Nature* **415,** 621–623 (2002).
20. Armani, D. K., Kippenberg, T. J., Spillane, S. M. & Vahala, K. J. Ultra-high-*Q* toroid microcavity on a chip. *Nature* **421,** 925–928 (2003).
21. Akahane, Y., Asano, T., Song, B. S. & Noda, S. High-*Q* photonic nanocavity in a two-dimensional photonic crystal. *Nature* **425,** 944–947 (2003).
22. Vahala, K. J. Optical microcavities. *Nature* **424,** 839–846 (2003).
23. Soljacic, M. & Joannopoulos, J. D. Enhancement of nonlinear effects using photonic crystals. *Nature Mater.* **3,** 211–219 (2004).
24. Yoshie, T. *et al.* Vacuum Rabi splitting with a single quantum dot in a photonic crystal nanocavity. *Nature* **432,** 200–203 (2004).
25. Kippenberg, T. J. & Vahala, K. J. Cavity optomechanics: back-action at the mesoscale. *Science* **321,** 1172–1176 (2008).
26. Shen, J. T., Catrysse, P. B. & Fan, S. Mechanism for designing metallic metamaterials with a high index of refraction. *Phys. Rev. Lett.* **94,** 197401 (2005).
27. Shin, J., Shen, J. T. & Fan, S. Three-dimensional metamaterials with an ultrahigh effective refractive index over a broad bandwidth. *Phys. Rev. Lett.* **102,** 093903 (2009).
28. Choi, M. *et al.* A terahertz metamaterial with unnaturally high refractive index. *Nature* **470,** 369–373 (2011).
29. Yao, J., Yang, X., Yin, X., Bartal, G. & Zhang, X. Three-dimensional nanometer scale optical cavities of indefinite medium. *Proc. Natl Acad. Sci. USA* **108,** 11327–11331 (2011).
30. Manalatou, C. *et al.* Coupling of modes analysis of resonant channel add–drop filters. *IEEE J. Quantum Electron.* **35,** 1322–1331 (1999).
31. Akahane, Y., Asano, T., Song, B. S. & Noda, S. Fine-tuned high-*Q* photonic-crystal nanocavity. *Opt. Express* **13,** 1202–1214 (2005).
32. Englund, D., Fushman, I. & Vuckovic, J. General recipe for designing photonic crystal cavities. *Opt. Express* **13,** 5961–5975 (2005).
33. Wheeler, H. A. Fundamental limitations of small antennas. *Proc. IRE* **35,** 1479–1484 (1947).

Acknowledgements

The authors acknowledge funding support from the US Department of Energy under contract no. DE-AC02-05CH11231 through Materials Sciences Division of Lawrence Berkeley National Laboratory (LBNL). J.S.R. acknowledges a fellowship from the Samsung Scholarship Foundation, Republic of Korea.

Author contributions

X.D.Y. and J.Y. performed numerical simulations. J.S.R. fabricated and SEM-imaged device samples. X.D.Y. carried out optical measurements. X.D.Y., X.B.Y. and X. Z. analysed the experimental data. X.D.Y., X.B.Y. and X.Z. wrote the manuscript. X.Z. and X.B.Y. guided the research. All authors contributed to discussions.

Additional information

The authors declare no competing financial interests. Supplementary information accompanies this paper at www.nature.com/naturephotonics. Reprints and permission information is available online at http://www.nature.com/reprints. Correspondence and requests for materials should be addressed to X.Z.